Spread of Correlations in Long-Range Interacting Quantum Systems

P. Hauke[1,2,*] and L. Tagliacozzo[3,†]

[1]Institute for Quantum Optics and Quantum Information, Austrian Academy of Sciences, A-6020 Innsbruck, Austria
[2]Institute for Theoretical Physics, University of Innsbruck, A-6020 Innsbruck, Austria
[3]ICFO—Institut de Ciencies Fotoniques, Avenue Carl Friedrich Gauss, 3 08860 Castelldefels, Barcelona, Spain

(Received 7 May 2013; published 12 November 2013)

The nonequilibrium response of a quantum many-body system defines its fundamental transport properties and how initially localized quantum information spreads. However, for long-range-interacting quantum systems little is known. We address this issue by analyzing a local quantum quench in the long-range Ising model in a transverse field, where interactions decay as a variable power law with distance $\propto r^{-\alpha}$, $\alpha > 0$. Using complementary numerical and analytical techniques, we identify three dynamical regimes: short-range-like with an emerging light cone for $\alpha > 2$, weakly long range for $1 < \alpha < 2$ without a clear light cone but with a finite propagation speed of almost all excitations, and fully nonlocal for $\alpha < 1$ with instantaneous transmission of correlations. This last regime breaks generalized Lieb-Robinson bounds and thus locality. Numerical calculation of the entanglement spectrum demonstrates that the usual picture of propagating quasiparticles remains valid, allowing an intuitive interpretation of our findings via divergences of quasiparticle velocities. Our results may be tested in state-of-the-art trapped-ion experiments.

DOI: 10.1103/PhysRevLett.111.207202 PACS numbers: 75.10.Pq, 03.65.Ud, 67.85.−d

Physics is about identifying which in nature are the causes and which are their effects. In abstract mathematical theories, however, this distinction is not always given. While special relativity was designed with the purpose of enforcing the causality principle, in nonrelativistic quantum mechanics none of the five postulates ensures causality. In that case, causality emerges as a consequence of the locality of interactions. By now we have been able to see causality at work in well-controlled quantum-mechanical experiments described by local Hamiltonians, such as ultracold atoms [1–3]. There, the spread of correlations is bounded by a light cone, similar to the spread of information in relativistic theories. However, experiments are currently set up where quantum dynamics under variable long-range interactions can be studied, e.g., in polar molecules [4–6], Rydberg atoms [7,8], or trapped ions [9–14]. This development makes it a pressing issue to answer the fundamental question: can the out-of-equilibrium dynamics of synthetic long-range Hamiltonians effectively break causality?

We address this issue by studying a model that is currently realized in trapped-ion experiments, the transverse Ising model with long-range interactions. As we will show, the out-of-equilibrium response to an initially localized perturbation explores, depending on the interaction range, three different degrees of locality breaking. Specifically, we characterize the out-of-equilibrium response [15] of the model to local quenches, obtained by perturbing locally the ground state of the system and observing its subsequent evolution.

When the Hamiltonian that drives the evolution consists of local terms, the initially localized perturbation spreads at a finite speed, leading to the formation of a characteristic light cone that bounds the propagation [1]. The reason for this behavior is the Lieb-Robinson bound [16], which in its essence formulates the principle of causality. Mathematically, under certain assumptions, the Lieb-Robinson bound expresses a bound for the time-dependent commutator between two operators $\mathcal{O}_A$, $\mathcal{O}_B(t)$, defined at $t = 0$ on two disjoint regions of the system A and B separated by a distance L [17,18],

$$[\mathcal{O}_A, \mathcal{O}'(t)_B] \leq \|\mathcal{O}_A\|\|\mathcal{O}'_B\| g(L) \frac{vt}{L}, \tag{1}$$

where on the right-hand side the norm is the operator norm, v is the Lieb-Robinson velocity, and $g(L)$ is an exponentially decaying function. This bound has proven essential for understanding the complexity of quantum states [17,18], allowing us to formulate several general theorems, e.g., connecting excitation gaps and decay of correlations [19,20].

In some systems, the Lieb-Robinson bound can be understood using an intuitive pseudoparticle picture [21–23]. This applies if the low-lying excitations can be obtained by populating (for translational invariant systems) different pseudoparticle momentum states, with the vacuum characterized by the absence of pseudoparticles. Then, the system responds to a local perturbation by emitting pseudoparticles propagating at different speeds. The fastest particles, which define the causal cone, propagate at a speed that is often identified as the Lieb-Robinson velocity for that specific model.

Much less is known about how correlations spread in the presence of long-range interactions, although these become important in many different contexts. Namely, in local models where some of the constituents propagate much faster than the others, one can capture the effect of

the fast constituents in an effective description of the slow ones involving a nonlocal interaction. A prime example is quantum electrodynamics, describing the contact interaction of charges with photons propagating at the speed of light. In the nonrelativistic limit, where the charges move much slower than the light, the presence of photons can be encoded in a long-range Coulomb potential between the charges. Theories with long-range interactions can have overextensive energies [24,25] and are thus strongly nonlocal. In such circumstances, one would expect that concepts like causality and the locality of quasiparticle excitations should be reconsidered.

The purpose of this Letter is to address this issue using complementary analytical and numerical calculations. We find three qualitatively different dynamical regimes, with a breakdown of Lieb-Robinson bounds for strong long-range interactions, and a weaker form of locality breaking that obeys the Lieb-Robinson bounds for intermediate interaction ranges. We are able to explain these regimes via the above-mentioned pseudoparticle picture. Finally, we discuss experimental regimes in trapped-ion setups where our findings can be observed.

For this purpose, we study the out-of-equilibrium dynamics generated by long-range interactions in the simplest possible scenario that can be implemented in trapped-ions experiments [26], namely the long-range transverse Ising chain (LRTI),

$$H = \sin(\theta)\sum_{\langle i,j\rangle}\frac{\sigma_i^x\sigma_j^x}{|i-j|^\alpha} + \cos(\theta)\sum_i \sigma_i^z. \qquad (2)$$

Here, σ denote the usual spin-1/2 Pauli matrices, and we set fundamental energy unit and lattice spacing to unity. We consider a finite chain of L sites with open boundary conditions. The parameter α is varied within the broad limits $3 \gtrsim \alpha \gtrsim 0$ that can be realized in the ion setups, allowing us to tune from effectively short-range to strong long-range physics. The parameter θ is varied in the range of antiferromagnetic interactions $0 \le \theta \le (\pi/2)$. For any $\alpha > 0$, the system has two gapped phases, a z-polarized phase for small θ, and a Néel-ordered phase for values of $\theta \simeq \pi/2$. The two phases are separated by a line of second-order phase transitions, whose universality class depends on α [27].

Although the LRTI model does not obey the bound (1), which only holds for exponentially decaying Hamiltonians, one can still find a generalized Lieb-Robinson bound [17,28,29] if the power-law interactions are reproducing. This condition, equivalent to a sufficiently fast decay, is fulfilled for $\alpha > 1$ (see the Supplemental Material [30]), and bounds decay of correlations by a power law governed by α.

Numerical results.—To study the effects of α on the out-of-equilibrium dynamics after a local quench, we use as initial state the ground state $|\psi_{\rm GS}\rangle$ of Hamiltonian (2) at specific values of θ and α, and at time $t = 0$ perturb it locally; typically $|\psi_0\rangle = \sigma^x_{L/2}|\psi_{\rm GS}\rangle$. To observe the response of $|\psi_{\rm GS}\rangle$ to this local perturbation, we evolve $|\psi_0\rangle$ in time with the same Hamiltonian (2).

In our analysis, we employ two complementary approaches, the quasiexact time-dependent variational principle (TDVP) on matrix-product states (MPS) [31] and a linear spin-wave theory (LSWT) (see the Supplemental Material [30]). The used TDVP algorithm generalizes the ones available in the literature [27,32–37]. Here, we consider chain sizes up to $L = 150$, and we have checked that the accuracy of MPS with matrix sizes $\chi \le 200$ is sufficient. The LSWT involves a higher degree of approximation, and is only valid for states with sufficient magnetic order. It has the advantage that it can access, with lower computational cost, larger times and system sizes than what is possible with the TDVP (we calculate numerically up to $L = 1024$ and analytically for the thermodynamic limit). In those regimes where the LSWT can be applied, we have checked that the two methods provide compatible results, showing that the time evolution they describe is essentially semiclassical. This agreement is plausible, since $|\psi_0\rangle$ contains a single excitation with a density that decreases during the evolution, thus justifying the assumption of noninteracting quasiparticles that underlies the LSWT.

We exemplify the TDVP results for $\theta = \pi/5$ [see Figs. 1(a)–1(c)], which is not accessible with the LSWT because a nearby quantum phase transition strongly reduces magnetic order. We study the spread of quantum correlations via the block entanglement entropy (EE) $\mathcal{S}_l = -\sum_n \rho_l^n \log \rho_l^n$, where ρ_l^n is the nth eigenvalue of the reduced density matrix ρ_l involving the spins $1, \ldots, l$. As known from Ref. [27], in the ground state of the

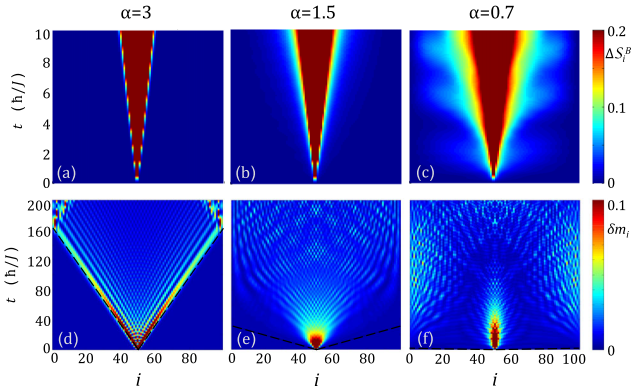

FIG. 1 (color online). (Non)light cones. (a)–(c) Block entanglement entropy $\Delta\mathcal{S}_l = \mathcal{S}_l(t) - \mathcal{S}_l(0)$ from the TDVP ($\theta = \pi/5$, $L = 100$). (d)–(f) Polarization $\delta m_i = \langle S_i^z\rangle + 1/2$ from the LSWT ($\theta = \pi/20$). (a),(d) For $\alpha > 2$, the excitation at $i = 50$ spreads light-cone-like, as in the short-range model. (b),(e) For $2 > \alpha > 1$, there is no well-defined wave front, but the excitation needs a finite time to bridge large distances. (c),(f) For $\alpha < 1$, the excitation spreads immediately over the entire system. Black dashed lines in (d),(e) denote the maximal spin-wave group velocity [in (f), it practically coincides with the abscissa].

z-polarized phase of the LRTI, the long-range interactions cause $\mathcal{S}_{L/2} \propto \log L$ when $\alpha < 2$. Therefore, to isolate the growth of the entropy generated during the time evolution, we analyze the excess of EE with respect to the initial state $\Delta\mathcal{S}_l = \mathcal{S}_l(t) - \mathcal{S}_l(0)$.

For the LSWT, we exemplify the resulting dynamics for $\theta = \pi/20$ [see Figs. 1(d)–1(f)], where the ground state is strongly polarized $\langle S_i^z \rangle \approx -1/2$ [27]. In this case, a useful measure for the spread of the perturbation is the excess magnetization $\delta m_i = \langle S_i^z \rangle + 1/2$. Notably, within the LSWT, this directly gives the single-site entanglement entropy $\mathcal{S}_i^{(1)} = (\delta m_i + 1)\log(\delta m_i + 1) - \delta m_i \log \delta m_i$ [38,39]. Figure 1 evidences the similar behavior for the two methods and the two θ regimes.

For generic θ, we identify three dynamical regimes as a function of α. (i) For $\alpha \geq 2$ [realized in nature, e.g., for van der Waals ($\alpha = 6$) or dipole-dipole ($\alpha = 3$) interactions], the system behaves as if short-range interacting, with an excitation maximum that defines a clear wave front. Its linear propagation gives a constant Lieb-Robinson velocity, coinciding with the maximal spin-wave group velocity. Outside the resulting light cone, correlations decay algebraically with a power determined by α, thus obeying the generalized Lieb-Robinson bounds. (ii) In the range $2 > \alpha > 1$, although at short times there appears an effect resembling a light cone, it does not really bound the propagation of the perturbation, since correlations consistently leak out of it, and at larger times one cannot identify a wave front. Further, we find complex interference effects due to longer-range spin flips. Still the excitation needs a finite time to bridge larger distances. (iii) For $\alpha < 1$ ($\alpha = 1$ corresponds to Coulomb- or gravitationlike potentials), the generalized Lieb-Robinson bounds valid for $\alpha > 1$ can no longer be defined. As a consequence, the system becomes truly long ranged, and correlations spread practically instantaneously over the chain.

These results complement the one of Ref. [40] about thermalization in disordered systems, where random interactions are modulated by a long-range power law. There, the time average of local observables tends to a value predicted by a generalized Gibbs ensemble only if $\alpha < 1$.

Our findings differ from previous results for the specific cases of Hamiltonians consisting of mutually commuting terms, such as Eq. (2) with $\theta = \pi/2$. In such settings, the block entropy of subsystems can increase unchecked with block size for $\alpha \leq 0.5$, whereas for $\alpha > 1$ it is strictly upper bounded [41]. Further, the value $\alpha = 0.5$ separates two dynamical regimes [42], one of which is characterized by prethermalization plateaus [43].

Pseudoparticle dispersion relation.—The qualitatively different behavior in the regimes (i)–(iii) can be understood in a simple quasiparticle picture: during the local quench, all spin-wave k modes become populated with occupation $\approx 1/L$. If the pseudoparticles do not interact (a good approximation for low pseudoparticle density), each mode subsequently propagates with its group velocity $v_g = (\partial\omega_k/\partial k)$, which depends only on the dispersion relation ω_k [cf. Fig. 2(a); see the Supplemental Material [30] for an analytical formula from the LSWT].

In the range $2 < \alpha < \infty$, the maximal group velocity $v_{\max}$ is achieved around $k = \pi/2$, and does barely depend on system size or α [see Fig. 2(b), top]. At $\alpha < 2$, however, ω_k acquires a cusp at $k = \pi$. Consequently, $v_{\max}$ is attained at $k = \pi \pm 2\pi/L$ [44]. It diverges as $v_{\max} \propto (2\pi/L)^{\alpha-2}$. Still, the time scale in which pseudoparticles can reach the boundary $t_b \equiv L/(2v_{\max})$ scales as $L^{\alpha-1}$, which diverges for $1 < \alpha \leq 2$; the time to reach the boundary increases with system size, even for the fastest mode.

The long-range effects become more dramatic at $\alpha < 1$ due to a stronger divergence $v_{\max} \propto (2\pi/L)^{(\alpha-3)/2}$. Now, for the fastest mode, t_b decreases with system size (actually for a diverging number of modes; see Fig. 2 and the Supplemental Material [30]). In Fig. 2(b), the transition between the three regimes can be clearly identified.

The spin-wave dispersion also explains the "diffusive" effect encountered at small α [see Figs. 1(e) and 1(f)]. With decreasing α, the dispersion becomes flatter around the sides of the Brillouin zone. Therefore, there are many slow quasiparticles that remain in the central region for a long time, giving rise to an apparent diffusive core of high density.

Scaling of entanglement entropy.—To numerically confirm the validity of the pseudoparticle picture, we analyze within the TDVP the increase of the EE of half of the chain $\mathcal{S}_{L/2}(t)$. Interestingly, for all values of α considered, the

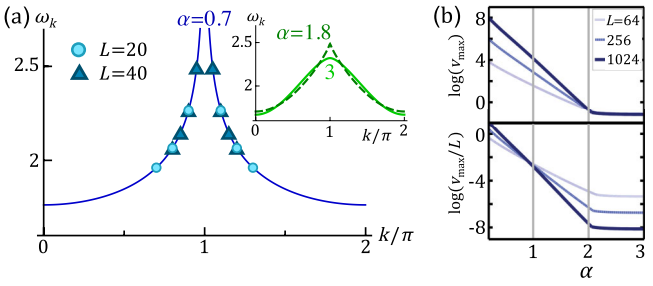

FIG. 2 (color online). (a) Spin-wave dispersion relations. Inset: for $\alpha > 2$, ω_k is a deformed cosine, similar to the short-range case, while at $\alpha < 2$, it develops a cusp at $k = \pi$, which becomes sharper with decreasing α. Main panel: for $\alpha < 1$, the number of modes with diverging group velocity $|v_g| > (L/2)/t_0$ increases with L for any $t_0 > 0$. Plot for $t_0 = 50$, with $L = 20$ (six modes with $|v_g| > (L/2)/t_0$, circles) and $L = 40$ (eight modes, triangles). (b) Maximal group velocity for different L (at $\theta = \pi/20$). Top: for $\alpha > 2$, $v_{\max}$ is essentially independent of α, while it increases sharply below $\alpha = 2$. Bottom: for $\alpha > 1$, $v_{\max}/L$ tends to zero for $L \to \infty$. The time $t_b \equiv L/(2v_{\max})$ at which excitations reach the system boundary diverges. For $\alpha < 1$, $v_{\max}/L$ increases with system size. Information about the local quench reaches the entire system instantaneously.

excess entropy $\Delta\mathcal{S}_{L/2}(t)$ initially increases as a power of t and then saturates to a value very close to $\Delta\mathcal{S}_{L/2}(t) = \log 2$, independent of system size [see Fig. 3(a)].

The initial growth is faster for smaller α, in agreement with the presence of faster pseudoparticles. Remarkably, due to these fast pseudoparticles the initial growth is stronger than logarithmic, which normally is considered the worst-case scenario, occurring at quenches to a critical point. Before entering the saturation regime, systems with smaller α start to evolve slower, in agreement with the appearance of a diffusive evolution. The fact that the excess of EE of a block saturates to a value independent of its size is in remarkable contrast to the ground-state properties. This effect finds a natural explanation in the semiclassical picture of pseudoparticles: the states that dominate the time evolution are states with only one pseudoparticle; the value $\Delta\mathcal{S}_{L/2} = \log 2$ is then immediately understood as coming from the two orthogonal possibilities of the pseudoparticle being either in the left or in the right half chain.

A further confirmation comes from the half-chain entanglement-spectrum evolution $h_n(L/2, t) = \log\rho^n_{L/2}(t)$, where $\rho^n_{L/2}$ is the nth eigenvalue of the reduced density matrix of half of the chain. The spectrum is dominated by only a few eigenvalues, with two of order 1 as expected from the log2 asymptote, and a huge number of eigenvalues below 10^{-5} [see Fig. 3(b)]. These eigenvalues grow steadily, but we expect that they do not affect equilibrium properties, since they are associated to higher energies and thus, at long times, their effect should average out. These findings are in agreement with similar observations in short-range systems

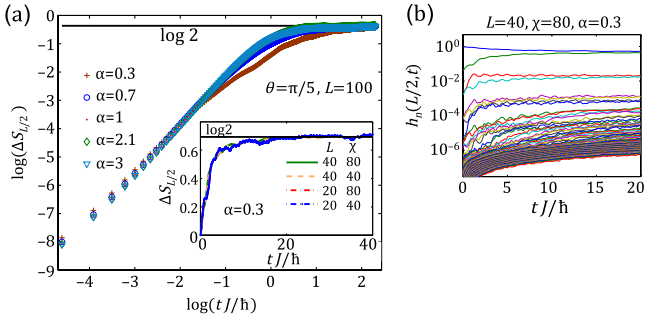

FIG. 3 (color online). (a) Growth of entanglement entropy. The excess $\Delta\mathcal{S}_{L/2}(t)$ grows initially as a power law with t for all considered α. It then saturates to log2 independent of system size, as expected from the pseudoparticle picture. This is shown in the insets where we compare the saturation value for chains of different length and for completeness show that there is no residual dependence of the saturation value on the MPS matrix dimension χ. (b) Evolution of the entanglement spectrum. The entanglement spectrum is dominated by two eigenvalues, which in the pseudoparticle picture correspond to the pseudoparticle being in the left or the right part of the chain. The other eigenvalues are significantly smaller, confirming the quality of semiclassical descriptions of the evolution.

[21,23,45–53], where semiclassical models provided a good description of these kinds of out-of-equilibrium dynamics.

Experimental implementation.—Due to their qualitative difference, the three dynamical regimes can be observed already in small experimental systems. A clear signature is, e.g., the speed with which excitations reach the boundary and its scaling with system size. Alternatively, the ratio of the wave-front maximum and the subsequent minimum distinguishes the short-range and the weakly long-range regime. In the former, it increases with system size, thus defining an increasingly sharp wave front. In the latter, it decreases until the wave front disappears.

Finally, let us remark that although the abstract LRTI model displays nonlocal behavior, an actual physical implementation will obey locality, as one would expect. For example, in the trapped-ion implementation, Hamiltonian (2) describes an effective dynamics for electronic states of the ions, which are coupled by collective phonon modes by employing laser fields [26,54,55]. The phonon dynamics can be neglected on time scales much larger than those associated to the detuning between laser driving and phonon frequencies. These time scales are typically $\mathcal{O}(10\ \mu\text{s})$. Moreover, the derivation of Eq. (2) employs a rotating-wave approximation in the phonon frequencies, corresponding to neglecting terms that average to zero on time scales $\mathcal{O}(1\ \mu\text{s})$. When the group velocity reaches these time scales, the effective Hamiltonian (2) breaks down, just as how the Coulomb potential is no longer valid when charged particles move close to the speed of light. On the other hand, the time scale of the spin interactions is typically $\hbar/J = \mathcal{O}(1\ \text{ms})$. Therefore, although the group velocities of the spin system cannot truly diverge, they can be several times larger than the scale set by J. This still provides a drastic effect that can be explored in typical practical implementations [9–14].

Conclusions.—Via quasiexact numerics based on tensor networks and analytical calculations of the spin-wave dispersion, we have identified three qualitatively different regimes of the nonequilibrium dynamics in the LRTI model, indicating different degrees of the breakdown of locality. The quasiparticle dispersion undergoes drastic changes at $\alpha = 2$ and $\alpha = 1$, marking a transition from short-range over weakly long-range to strong long-range physics. In the last case, diverging quasiparticle velocities lead to a practically instantaneous spread of excitations through the entire system. These regimes are independent of the underlying ground-state phase. It will be interesting to study how these findings carry over to larger dimensions. Finally, we have outlined how to identify the different degrees of nonlocality in typical trapped-ion experiments, and we hope our findings will inspire experiments along these lines.

Identifying violations of the Lieb-Robinson bounds—besides establishing the presence or absence of causality in systems with long-range interactions—may pave the way for extending well-established results about the complexity of ground states [17,18], and the relation between the

decay of correlations and the scaling of entanglement [19,20]. Moreover, the Lieb-Robinson bound has important implications for thermalization [56,57]: if the system locally equilibrates to a generalized Gibbs ensemble, time-dependent correlation functions are described by the same ensemble [58]. These are key issues that have strong technical consequences for our ability to simulate the quantum system on a computer. Indeed, simulations based on tensor networks such as MPS, or the multiscale entanglement renormalization ansatz (MERA), typically require a small amount of entanglement—but due to Lieb-Robinson bounds, correlations build up linearly during time evolution, making numerical simulations often unfeasible [59].

We acknowledge interesting discussions with P. Calabrese, J. Eisert, Th. Koffel, C. Laflamme, B. Lanyon, M. Lewenstein, F. Verstraete, and P. Zoller, and financial support from the Marie Curie Project No. FP7-PEOPLE-2010-IIF ENGAGES Grant No. 273524, TOQATA (Grant No. FIS2008-00784), Spanish MICINN (Grant No. FIS2008-00784), Catalunya-Caixa, the Austrian Science Fund (Grant No. SFB F40 FOQUS), EU IP SIQS, and the DARPA OLE program.

Note added.—During the review process for this Letter, two related articles appeared, one that studies the LRTI under global quenches [61], and one that studies local quenches in a LRTI with interactions modeled after a realistic trapped-ion string with nonuniform interion distances [62]. Both obtain a transition of dynamical behavior [63,64] at the same value $\alpha = 1$ as this Letter.

*philipp.hauke@uibk.ac.at
†luca.tagliacozzo@icfo.es

[1] M. Cheneau, P. Barmettler, D. Poletti, M. Endres, P. Schausz, T. Fukuhara, C. G. Christian, I. Bloch, C. Kollath, and S. Kuhr, Nature (London) **481**, 484 (2012).
[2] S. Trotzky, Y.-A. Chen, A. Flesch, I. P. McCulloch, U. Schollwöck, J. Eisert, and I. Bloch, Nat. Phys. **8**, 325 (2012).
[3] J. P. Ronzheimer, M. Schreiber, S. Braun, S. S. Hodgman, S. Langer, I. P. McCulloch, F. Heidrich-Meisner, I. Bloch, and U. Schneider, Phys. Rev. Lett. **110**, 205301 (2013).
[4] T. Lahaye, C. Menotti, L. Santos, M. Lewenstein, and T. Pfau, Rep. Prog. Phys. **72**, 126401 (2009).
[5] L. D. Carr, D. DeMille, R. V. Krems, and J. Ye, New J. Phys. **11**, 055049 (2009).
[6] C. Trefzger, C. Menotti, B. Capogrosso-Sansone, and M. Lewenstein, J. Phys. B **44**, 193001 (2011).
[7] M. Saffman, T. G. Walker, and K. Mølmer, Rev. Mod. Phys. **82**, 2313 (2010).
[8] R. Löw, H. Weimer, J. Nipper, J. B. Balewski, B. Butscher, H.-P. Büchler, and T. Pfau, J. Phys. B **45**, 113001 (2012).
[9] A. Friedenauer, H. Schmitz, J. T. Glueckert, D. Porras, and T. Schaetz, Nat. Phys. **4**, 757 (2008).
[10] K. Kim, M.-S. Chang, S. Korenblit, R. Islam, E. E. Edwards, J. K. Freericks, G.-D. Lin, L.-M. Duan, and C. Monroe, Nature (London) **465**, 590 (2010).
[11] R. Islam, E. Edwards, K. Kim, S. Korenblit, C. Noh, H. Carmichael, G.-D. Lin, L.-M. Duan, C.-C. J. Wang, J. Freericks, and C. Monroe, Nat. Commun. **2**, 377 (2011).
[12] B. P. Lanyon, C. Hempel, D. Nigg, M. Müller, R. Gerritsma, F. Zähringer, P. Schindler, J. T. Barreiro, M. Rambach, G. Kirchmair, M. Hennrich, P. Zoller, R. Blatt, and C. F. Roos, Science **334**, 57 (2011).
[13] R. Islam, C. Senko, W. C. Campbell, S. Korenblit, J. Smith, A. Lee, E. E. Edwards, C.-C. J. Wang, J. K. Freericks, and C. Monroe, Science **340**, 583 (2013).
[14] J. W. Britton, B. C. Sawyer, A. C. Keith, C.-C. J. Wang, J. K. Freericks, H. Uys, M. J. Biercuk, and J. J. Bollinger, Nature (London) **484**, 489 (2012).
[15] A. Polkovnikov, K. Sengupta, A. Silva, and M. Vengalattore, Rev. Mod. Phys. **83**, 863 (2011).
[16] E. Lieb and D. Robinson, Commun. Math. Phys. **28**, 251 (1972).
[17] M. B. Hastings, in *Quantum Theory from Small to Large Scales*, Lecture Notes of the Les Houches Summer School Vol. 95, edited by J. Frohlich, M. Salmhofer, V. Mastropietro, W. De Roeck, and L. F. Cugliandolo (Oxford University Press, Oxford, UK, 2010).
[18] B. Nachtergaele and R. Sims, IAMP News Bull., 22 (2010).
[19] M. B. Hastings, J. Stat. Mech. (2007) P08024.
[20] L. Masanes, Phys. Rev. A **80**, 052104 (2009).
[21] P. Calabrese and J. Cardy, J. Stat. Mech. (2005) P04010.
[22] P. Calabrese and J. Cardy, Phys. Rev. Lett. **96**, 136801 (2006).
[23] P. Calabrese and J. Cardy, J. Stat. Mech. (2007) P10004.
[24] D. Mukamel, in *Long-Range Interacting Systems*, Lecture Notes of the Les Houches Summer School Vol. 90, edited by T. Dauxois, S. Ruffo, and L. F. Cugliandolo (Oxford University Press, Oxford, UK, 2008).
[25] A. Campa, T. Dauxois, and S. Ruffo, Phys. Rep. **480**, 57 (2009).
[26] D. Porras and J. I. Cirac, Phys. Rev. Lett. **92**, 207901 (2004).
[27] T. Koffel, M. Lewenstein, and L. Tagliacozzo, Phys. Rev. Lett. **109**, 267203 (2012).
[28] M. B. Hastings and T. Koma, Commun. Math. Phys. **265**, 781 (2006).
[29] M. Cramer and A. Serafini, and J. Eisert, in *Quantum Information and Many Body Quantum Systems*, edited by M. Ericsson and S. Montangero (Edizioni della Normale, Pisa, 2008), pp. 51–72.
[30] See Supplemental Material at http://link.aps.org/supplemental/10.1103/PhysRevLett.111.207202 for details on the TDVP, the LSWT, and reproducing functions.
[31] M. C. Banuls, M. B. Hastings, F. Verstraete, and J. I. Cirac, Phys. Rev. Lett. **102**, 240603 (2009).
[32] G. M. Crosswhite, A. C. Doherty, and G. Vidal, Phys. Rev. B **78**, 035116 (2008).
[33] I. P. McCulloch, arXiv:0804.2509.
[34] F. Fröwis, V. Nebendahl, and W. Dür, Phys. Rev. A **81**, 062337 (2010).
[35] J. Haegeman, J. I. Cirac, T. J. Osborne, I. Pizorn, H. Verschelde, and F. Verstraete, Phys. Rev. Lett. **107**, 070601 (2011).
[36] V. Nebendahl and W. Dür, Phys. Rev. B **87**, 075413 (2013).

[37] A. Milsted, J. Haegeman, T. J. Osborne, and F. Verstraete, Phys. Rev. B **88**, 155116 (2013).
[38] I. Peschel and V. Eisler, J. Phys. A **42**, 504003 (2009).
[39] H. F. Song, N. Laflorencie, S. Rachel, and K. Le Hur, Phys. Rev. B **83**, 224410 (2011).
[40] S. Ziraldo and G. E. Santoro, Phys. Rev. B **87**, 064201 (2013).
[41] W. Dür, L. Hartmann, M. Hein, M. Lewenstein, and H. J. Briegel, Phys. Rev. Lett. **94**, 097203 (2005).
[42] R. Bachelard and M. Kastner, Phys. Rev. Lett. **110**, 170603 (2013).
[43] M. van den Worm, B. C. Sawyer, J. J. Bollinger, and M. Kastner, New J. Phys. **15**, 083007 (2013).
[44] $v_g(k = \pi)$ is not well defined and is set to 0.
[45] V. Eisler and I. Peschel, J. Stat. Mech. (2007) P06005.
[46] V. Eisler, D. Karevski, T. Platini, and I. Peschel, J. Stat. Mech. (2008) P01023.
[47] Á. Perales and G. Vidal, Phys. Rev. A **78**, 042337 (2008).
[48] A. M. Läuchli and C. Kollath, J. Stat. Mech. (2008) P05018.
[49] M. Fagotti and P. Calabrese, Phys. Rev. A **78**, 010306(R) (2008).
[50] F. Iglói, Z. Szatmári, and Y.-C. Lin, Phys. Rev. B **80**, 024405 (2009).
[51] H. Rieger and F. Iglói, Phys. Rev. B **84**, 165117 (2011).
[52] J.-M. Stéphan and J. Dubail, J. Stat. Mech. (2011) P08019.
[53] F. Iglói, Z. Szatmári, and Y.-C. Lin, Phys. Rev. B **85**, 094417 (2012).
[54] D. Porras and J. Cirac, Phys. Rev. Lett. **96**, 250501 (2006).
[55] C. Schneider, D. Porras, and T. Schaetz, Rep. Prog. Phys. **75**, 024401 (2012).
[56] T. Kinoshita, T. Wenger, and D. S. Weiss, Nature (London) **440**, 900 (2006).
[57] M. Rigol, V. Dunjko, V. Yurovsky, and M. Olshanii, Phys. Rev. Lett. **98**, 050405 (2007).
[58] F. H. L. Essler, S. Evangelisti, and M. Fagotti, Phys. Rev. Lett. **109**, 247206 (2012).
[59] Recent extensions to the branching MERA suggest that such limitations might eventually be overcome [60].
[60] G. Evenbly and G. Vidal, arXiv:1210.1895.
[61] J. Schachenmayer, B. P. Lanyon, C. F. Roos, and A. J. Daley, Phys. Rev. X **3**, 031015 (2013).
[62] Z.-X. Gong and L.-M. Duan, arXiv:1305.0985.
[63] R. Schützhold, J. Low Temp. Phys. **153**, 228 (2008).
[64] M. Heyl, A. Polkovnikov, and S. Kehrein, Phys. Rev. Lett. **110**, 135704 (2013).